

Interaction of U-box E3 ligase SNEV with PSMB4, the $\beta 7$ subunit of the 20 S proteasome

Marlies LÖSCHER*, Klaus FORTSCHEGGER*, Gustav RITTER*, Martina WOSTRY*, Regina VOGLAUER*, Johannes A. SCHMID†, Steven WATTERS‡, A. Jennifer RIVETT‡, Paul AJUH§, Angus I. LAMOND§, Hermann KATINGER* and Johannes GRILLARI*||¹

*Institute of Applied Microbiology, University of Natural Resources and Applied Life Sciences, Muthgasse 18, A-1190 Vienna, Austria, †Department of Vascular Biology and Thrombosis Research, University of Vienna, Brunnerstrasse 59, A-1235 Vienna, Austria, ‡The Department of Biochemistry, School of Medical Sciences, University of Bristol, University Walk, Bristol BS8 1TD, U.K., §Division of Gene Regulation and Expression, Wellcome Trust Biocentre, University of Dundee, Dow Street, Dundee DD1 5EH, U.K., and ||BMT Biomolecular Therapeutics, Brunnerstrasse 59, Vienna, Austria

Recognition of specific substrates for degradation by the ubiquitin–proteasome pathway is ensured by a cascade of ubiquitin transferases E1, E2 and E3. The mechanism by which the target proteins are transported to the proteasome is not clear, but two yeast E3s and one mammalian E3 ligase seem to be involved in the delivery of targets to the proteasome, by escorting them and by binding to the 19 S regulatory particle of the proteasome. In the present study, we show that SNEV (senescence evasion factor), a protein with *in vitro* E3 ligase activity, which is also involved in DNA repair and splicing, associates with the proteasome by directly binding to the $\beta 7$ subunit of the 20 S proteasome. Upon inhibition of proteasome activity, SNEV does not accumulate within the cells although its co-localization with the proteasome increases significantly. Since immunofluorescence microscopy

also shows increased co-localization of SNEV with ubiquitin after proteasome inhibition, without SNEV being ubiquitinated by itself, we suggest that SNEV shows E3 ligase activity not only *in vitro* but also *in vivo* and escorts its substrate to the proteasome. Since the yeast homologue of SNEV, Prp19, also interacts with the yeast $\beta 7$ subunit of the proteasome, this mechanism seems to be conserved during evolution. Therefore these results support the hypothesis that E3 ligases might generally be involved in substrate transport to the proteasome. Additionally, our results provide the first evidence for a physical link between components of the ubiquitin–proteasome system and the spliceosome.

Key words: Pre4, Prp19, PSMB4, 20 S proteasome, senescence evasion factor (SNEV), spliceosome.

INTRODUCTION

The proteasome is a large multisubunit protease which is ubiquitous to life and plays a crucial role in intracellular protein degradation [1]. Proteasomes of eukaryotes have a complex structure that has been elucidated at the molecular level recently [2]. They comprise a barrel-shaped catalytic 20 S proteasome core complex, capped at both poles by a 19 S regulatory ATPase complex. This association with the 19 S cap complex [3] forms the 26 S proteasome, which controls substrate accession to the proteases and enhances the proteolytic activity of the core in an energy-dependent manner.

The 26 S proteasome is a dynamic structure having multiple interactions with transiently associated subunits and cellular factors that are necessary for functions such as cellular localization, presentation of substrates, substrate-specific interactions and generation of various products [3]. Degradation of proteins by the proteasome in the cell depends on their recognition, labelling and transport to it.

A multistep process leads to the transfer of ubiquitin or multi-ubiquitin chains on to a substrate. This process includes activation of ubiquitin by an E1 enzyme and transfer of this ubiquitin to an E2 ubiquitin-conjugating enzyme that in turn transfers the ubiquitin moiety to an E3 ligase or in concert with an E3 ligase to the substrate. The lysine residue by which the ubiquitin chains are linked together is an important signal that determines the fate of the

substrate; Lys⁴⁸ linkage for example is the major signal that targets proteins for destruction to the proteasome [4].

We have identified SNEV (senescence evasion factor; hNMP200, Prp19-like, hPso4; NCBI accession no. NP_055317; unknown gene 4 [5]) in a screening for differentially expressed genes in early passage and replicatively senescent human endothelial cells. SNEV is also involved in the regulation of cellular life span (R. Voglauer, W. M. F. Chang, M. Wieser, K. Baumann, H. Katinger and J. Grillari, unpublished work). Additionally, it is a part of the spliceosome-associated complex [6], localized in the nucleus [7] and involved in DNA double-strand break repair [8].

SNEV displays E3 ubiquitin ligase activity *in vitro* [9]. This activity is dependent on its U-box domain and on the E2 enzyme UbcH3. Since multiubiquitin chains that are linked by Lys⁴⁸ are formed in this *in vitro* assay, it is suggested that SNEV confers the ‘classical’ signal for protein degradation by the proteasome (reviewed in [4]).

Since yeast E3 enzymes have been reported to transport their substrates to, and to interact with, the proteasome [10,11], we were interested to know whether this is a general and conserved mechanism valid also in mammalian cells. One indication that this might be true for SNEV, is the report that the $\beta 7$ subunit of the *Caenorhabditis elegans* proteasome pulled out the homologue of SNEV in a Y2H (yeast two-hybrid) high-throughput screening ([12] electronic supplement).

Abbreviations used: AD, activation domain; BD, binding domain; CFP, cyan fluorescent protein; CoIP, co-immunoprecipitation; ECFP, enhanced CFP; YFP, yellow fluorescent protein; EYFP, enhanced YFP; FRET, fluorescence resonance energy transfer; GST, glutathione S-transferase; HA, haemagglutinin; HEK-293 cell, human embryonic kidney 293 cell; I κ B α , inhibitory κ B α ; Ni²⁺-NTA, Ni²⁺-nitrilotriacetate; SD, synthetic dropout; SNEV, senescence evasion factor; Y2H, yeast two-hybrid.

¹ To whom correspondence should be addressed, at Muthgasse 18, A-1190, Vienna, Austria (email j.grillari@iam.boku.ac.at).

Table 1 Primers used in this study

Underlined sequences indicate the restriction sites that were used for ligation into plasmids.

Primer name	Sequence
SNEV sense	5'-GTAGAATTCATGTCCTAATCTGCTCCATC-3'
SNEV antisense	5'-ATACAAGTCGACCTACTGAGATGAGGCCAGC-3'
SNEV(Δ WD40) antisense	5'-ATACAAGTCGACCTGAGCTCTTCTGGCTTC-3'
SNEV(WD40) sense	5'-GTAGAATTCAAATACCGGCAGGTGGCATC-3'
SNEV(Δ U67) sense	5'-GTAGAATTCACGCCACCAGCATCCCG-3'
SNEV(Δ U90) sense	5'-GTAGAATTCACTCTGCGCCAGCAGCTG-3'
PRE4 sense	5'-GATCGAATTCATGAATCAGCATCTTTTCAG-3'
PRE4 antisense	5'-GATCCTCGAGCTAAATTTTTGAGTACCGT-3'
PSMB4 sense	5'-GATCGAATTCATGGAAGCGTTTTGGGGTC-3'
PSMB4 antisense	5'-GATCCTCGAGTCATCAAGCCACTGATCATG-3'
PSMB4(PP) antisense	5'-GATCCTCGAGCCGCGTGATTGGACCTCTG-3'
PSMB4(P122) antisense	5'-GATCCTCGAGTCCATCTCCAGAAAGCTCCT-3'
PSMB4(P Δ 102) sense	5'-GATCGAATTCACGCTGATTTCCAGTATT-3'
PSMB4-wo-PP sense	5'-GATCGAATTCATGACCCAGAACCCCATGGTAC-3'
PSMB4(P101) antisense	5'-GATCCTCGAGCAAATACTGGAATCAGCGTAGTC-3'
PSMB4(P Δ 122) sense	5'-GATCGAATTCGGAGATGACACAGCTATAG-3'
deltaU66senseXhoI_C1	5'-ATCACTCGAGCTATGTCAGCCACCAGCATCCCG-3'
deltaU89senseXhoI_C1	5'-ATCACTCGAGCTATGACTCTGCGCCAGCAGCTG-3'

In the present study, we show that SNEV indeed interacts with the proteasome. The interaction is direct and evolutionarily conserved from yeast to human and the interacting partner of SNEV is the $\beta 7$ subunit (PSMB4) of the 20 S proteasome. Although the 19 S cap has been known to bind components of the ubiquitin system, this is the first report that the 20 S core has the same ability. These findings therefore support the idea that interaction of E3 ligase with the proteasome might be a general mechanism to either target the proteasome to the sites of protein degradation or to target and escort the ubiquitinated proteins to the sites of destruction.

MATERIALS AND METHODS

Sequence comparison and structure of $\beta 7$ 20 S subunit

Sequence comparisons of *Homo sapiens* SNEV (NCBI accession no. NP_055317) and *Saccharomyces cerevisiae* Prp19 (NCBI accession no. NP_013064), SNEV and *C. elegans* T10F2.4 (NCBI accession no. AAK21467), *H. sapiens* PSMB4 (NCBI accession no. NP_002787) and *S. cerevisiae* Pre4 (NCBI accession no. NP_116708) and PSMB4 and *C. elegans* pbs-7 (NCBI accession no. NP_492354) were performed using the GenBank® database [13]. Additionally, species sequence comparison of human, yeast and worm homologues was performed using LaserGene, 4.0 (DNASTAR, Madison, WI, U.S.A.). The structure of the bovine $\beta 7$ 20 S subunit (PDB accession no. 1IRU), integrated within the proteasome, was modelled using Swiss-PdbViewer 3.7 [14] and the structure of yeast Pre4 (PDB accession no. 1FNT), integrated within the proteasome, was modelled using RasMol Version 2.6-beta-2 [15].

Construction of plasmids

General methods like PCR, transformation of *Escherichia coli* cells, restriction reactions, DNA ligations and other recombinant DNA techniques were performed following standard procedures [16]. In brief, the coding sequences of SNEV and PSMB4 were amplified by RT-PCR. Total RNA was prepared using Trizol® reagent (Invitrogen, Carlsbad, CA, U.S.A.). Total RNA (1 μ g) from HUVEC (human umbilical-vein endothelial cells) was reverse-transcribed using oligo(dT)₂₅ primers, and standard PCR with the primers described in Table 1 was performed. Prp19

and Pre4 were directly amplified by PCR using genomic DNA from the yeast strain W303 as a template. Primer sequences are shown in Table 1. The inserts were ligated into pGADT7 and pGBKT7 for Y2H analysis, into pEYFP-C1, pEYFP-N1, pECFP-C1 and pECFP-N1 for FRET (fluorescence resonance energy transfer) analysis (ClonTech Laboratories, Palo Alto, CA, U.S.A.) and into pGEX-6P-1 (Amersham Biosciences, Uppsala, Sweden) for GST (glutathione S-transferase) pull-down assays. All plasmid constructs were amplified in *E. coli* and the inserts were confirmed to contain no mutations by sequence analysis. The His₆-SNEV-containing plasmid for baculoviral expression was kindly provided by S. Hatakeyama.

Y2H assays

Screening for SNEV-interacting proteins was performed using the MATCHMAKER GAL4 Two-Hybrid System3 (ClonTech Laboratories) according to the manufacturer's guidelines. Therefore the cDNAs of SNEV and SNEV deletion constructs: SNEV(Δ WD40) amino acids 1–205, SNEV(WD40) amino acids 206–504, SNEV(Δ U67) amino acids 67–504, SNEV(Δ U90) amino acids 91–504 and SNEV(U96) as well as Pre4 cDNAs were inserted into the bait vector pGBKT7 (ClonTech Laboratories) in frame with the GAL4 DNA BD (binding domain) and a c-Myc epitope. PSMB4 and its deletion mutants: PSMB4(PP) propeptide amino acids 1–45, PSMB4(P122) amino acids 1–122, PSMB4(P Δ 102) amino acids 102–264, PSMB4(P101) amino acids 1–101, PSMB4(P Δ 122) amino acids 123–264 as well as Prp19 were inserted into the vector pGADT7 (ClonTech Laboratories) providing the GAL4 AD (activation domain) and the HA (haemagglutinin) tag. All constructs were amplified in *E. coli* and sequence analysed to confirm correct proteins. Then the constructs were introduced into *S. cerevisiae* strain AH109 (ClonTech Laboratories) by LiAc-co-transformation [17]. We selected interaction-positive clones by growth on high stringency SD (synthetic dropout) medium (4 \times SD: – Trp/– Leu/– His/– Ade; four times the SD medium lacking the amino acids tryptophan, leucine, histidine and the nucleotide adenine).

In vitro CoIP (co-immunoprecipitation)

Seize primary immunoprecipitation kit (Pierce, Rockford, IL, U.S.A.) was used to couple the c-Myc-tag antibody (ClonTech Laboratories) to agarose beads according to the manufacturer's guidelines. *In vitro* translation of SNEV, PSMB4 and Pre4 was performed using the pGADT7- and pGBKT7-derived plasmids as templates, and thus c-Myc-/HA-tagged proteins were synthesized using TNT Quick Coupled Transcription/Translation System (Promega, Madison, WI, U.S.A.). SNEV and PSMB4 proteins were labelled with ³⁵S-methionine (Amersham Biosciences). After mixing the *in vitro* translates and incubating at 37°C for 1 h, precipitation was performed by addition of the c-Myc-tag antibody-coupled beads and incubation at room temperature (22°C) for 3 h in binding buffer [20 mM Tris/HCl (pH 7.4), 140 mM NaCl, 10% (v/v) glycerol, 1 mM CaCl₂, 0.1% Triton X-100; and one tablet of Complete protease inhibitor cocktail (Roche, Basel, Switzerland) to 50 ml of buffer]. The beads were washed four times in binding buffer and elution was achieved by heating for 10 min in SDS sample buffer. After SDS/PAGE analysis, according to standard procedures [16], the gel was fixed, dried and proteins were detected by autoradiography.

For CoIP of Prp19–His₆ and Myc–Pre4 (*in vitro* translated), Prp19–His₆ cloned into pYPGE15 vector and transformed into yeast strain MG5128 (J. Grillari, G. Stadler and M. Grey, unpublished work) was grown overnight in 10 ml of SD/– Ura medium.

The yeast cells were harvested by centrifugation and washed three times in breaking buffer (50 mM sodium phosphate, pH 7.4, 1 mM PMSF, 1 mM EDTA and 5% glycerol). After another centrifugation, the cells were resuspended in SET buffer (1 M Sorbitol, 10 mM Tris/HCl, pH 8.0, and 50 mM EDTA), mixed on a vortex and incubated for 30 min at 37°C. The pellet was again resuspended in breaking buffer containing 1% Na₃N, 1% EDTA and 1% PMSF. Lysis was performed by an addition of glass beads and six cycles of 30 s mixing on a vortex and 30 s of incubation on ice.

CoIP was performed by incubation of the Prp19–His₆-containing yeast cell lysate and *in vitro* translated c-Myc–Pre4 protein for 1 h at 4°C, followed by an incubation with Ni²⁺-NTA (Ni²⁺-nitrilotriacetate) agarose beads (Qiagen, Hilden, Germany) for 1.5 h at 4°C. The beads were pre-equilibrated with TBST buffer (150 mM NaCl, 20 mM Tris/HCl, pH 7.5, and 0.1% v/v, Tween 20). Then the beads were washed five times with TBST buffer and elution was performed by heating for 10 min with SDS/PAGE sample buffer. After SDS/PAGE, precipitated Pre4 was detected using anti-c-Myc antibody (ClonTech Laboratories) and anti-mouse peroxidase conjugate as secondary antibody (Sigma–Aldrich, St. Louis, MO, U.S.A.).

GST pull-down assay

Mature PSMB4 (without propeptide) was cloned into pGEX-6P-1 as a GST-fusion, then transformed into *E. coli* BL21 and expressed using Overnight Express Autoinduction System 1 (Novagen, Darmstadt, Germany). Purification was performed using the Micro Spin GST Purification Module (Amersham Biosciences) according to the manufacturer's instructions. His₆-SNEV was expressed in Sf9 insect cells and affinity-purified on a Ni²⁺-NTA column (E. Böhm, J. Grillari, S. Gross, W. Ernst, B. Ferko, N. Borth and H. Katinger, unpublished work). For the pull-down assay, equal amounts of the purified proteins (0.5 µg) were mixed together and incubated for 2 h at 4°C in CoIP buffer (200 mM NaCl, 25 mM Tris/HCl, pH 7.4, and 0.5% Triton X-100). After that, glutathione–Sepharose 4B beads (Amersham Biosciences), equilibrated with CoIP buffer, were added, followed by incubation for 2 h at 4°C. Then the beads were washed three times with CoIP buffer and proteins were eluted with SDS/PAGE sample buffer. After SDS/PAGE, precipitated SNEV was detected using anti-His₆ antibody (Qiagen). GST was detected using anti-GST antibody (Amersham Biosciences) and anti-goat peroxidase conjugate as secondary antibody (Sigma–Aldrich).

Cell culture

HeLa cells were grown in DMEM (Dulbecco's modified Eagle's medium) supplemented with 4 mM L-glutamine and 10% (v/v) foetal calf serum. HEK-293 (human embryonic kidney 293) cell line was grown in DMEM/Ham's medium supplemented with 4 mM L-glutamine and 10% foetal calf serum. Proteasome activity of HeLa cells was blocked using 25 µM MG132 (Calbiochem, Darmstadt, Germany) in the medium.

Cell lysis for Western blots

Cells were lysed in 50 ml of nuclear lysis buffer containing 50 mM Tris (pH 7.5), 0.5 M NaCl, 1% Nonidet P40, 1% deoxycorticosterone, 0.1% SDS, 2 mM EDTA and 1 Complete protease inhibitor tablet (Roche Diagnostics, Vienna, Austria). Proteins were detected using anti-SNEV antibody Prp19–866, anti-p53 antibody (BP53-12; Sigma–Aldrich), anti-β-actin antibody (Sigma–Aldrich) and anti-ubiquitin antibody (MBL International, Woburn, MA, U.S.A.).

In vitro 26 S proteasome degradation assay

His₆-SNEV (0.3 µg) was incubated in the presence and in the absence of 0.3 µg of 26 S proteasome, purified from rat liver as described previously [19], for 2 h at 37°C. Reactions were performed in 50 mM Hepes buffer (pH 7.5) containing 5 mM ATP and 5 mM MgCl₂. At various time points, aliquots were added to SDS/PAGE gel sample buffer and heated at 100°C for 5 min and then frozen. For analysis, SDS/PAGE and Western blotting were performed. IκBα (inhibitory κBα) was used as a model substrate to confirm the activity of proteasome and was detected in Western blots using an anti-IκBα antibody (sc-1643; Santa Cruz Biotechnology, Santa Cruz, CA, U.S.A.). Densitometry was performed using an imaging densitometer (Model GS-690; Bio-Rad, Hercules, CA, U.S.A.).

In vivo CoIP

For proteasome preparation, HEK-293 cells were lysed in CoIP lysis buffer (20 mM Tris, pH 7.5, 10% glycerol, 5 mM ATP and 0.2% Nonidet P40). The lysate was added to anti-α2 20 S subunit antibody-coupled Protein A–agarose beads (Roche Diagnostics, Vienna, Austria) (coupling in 1 × PBS, 3 h at 4°C) and incubated overnight at 4°C. As control, anti-c-Myc antibody was coupled on to agarose beads and incubated with HEK-293 cell lysate as described above. The beads were washed four times with CoIP washing buffer (50 mM Tris, pH 7.5, 10% glycerol, 5 mM ATP, 150 mM NaCl and 0.2% Triton X-100) and resuspended in SDS loading buffer. SNEV and PSMB4 were detected by Western-blot analysis using anti-PSMB4 antibody (Affiniti Research, Mamhead Castle, Mamhead, Exeter, Devon, U.K.) and anti-SNEV antibody Prp19–866 with anti-rabbit peroxidase conjugate as secondary antibody (Sigma–Aldrich). Co-precipitated Cdc5L was detected by rabbit anti-Cdc5L antibody.

FRET

SNEV, SNEVΔ66, SNEVΔ89 and PSMB4 inserted into pECFP-N1, pECFP-C1 and pEYFP-N1, pEYFP-C1 respectively were transiently co-transformed into COS-1 and HEK-293 cells by Lipofectamine™ 2000 (Invitrogen) according to the manufacturer's guidelines. After 24 h, FRET images from living cells were generated by the MicroFRET method as described by Youvan et al. [20]. Photos were captured on a Nikon Diaphot TMD microscope with a cooled charge-coupled device camera (Kappa GmbH, Gleichen, Germany), with the YFP (yellow fluorescent protein), CFP (cyan fluorescent protein) and FRET filter sets (Omega Optical, Brattleboro, VT, U.S.A.), under identical conditions and processed with Scion Image software version beta 4.0.2 (Scion, Frederick, MD, U.S.A.). The images were aligned by pixel shifting, inverted, and the background was subtracted. Images from the YFP and CFP filter sets were multiplied with their previously assessed correction factors (0.19 for YFP and 0.59 for CFP) and subtracted from the FRET filter set picture. The remaining signals were multiplied by 3 for better visualization and they represent the corrected FRET.

Cell staining and immunofluorescence analyses

HeLa cells were washed with PBS and fixed for 5 min in 3.7% (w/v) paraformaldehyde in CSK buffer (10 mM Pipes, pH 6.8, 10 mM NaCl, 300 mM sucrose, 3 mM MgCl₂ and 2 mM EDTA) at room temperature. Permeabilization was performed with 1% Triton X-100 in PBS for 15 min at room temperature. Cells were incubated with primary antibodies diluted in PBS with 1% (v/v) goat serum for 1 h, washed three times with PBS for 10 min, incubated for 1 h with the appropriate secondary antibodies diluted

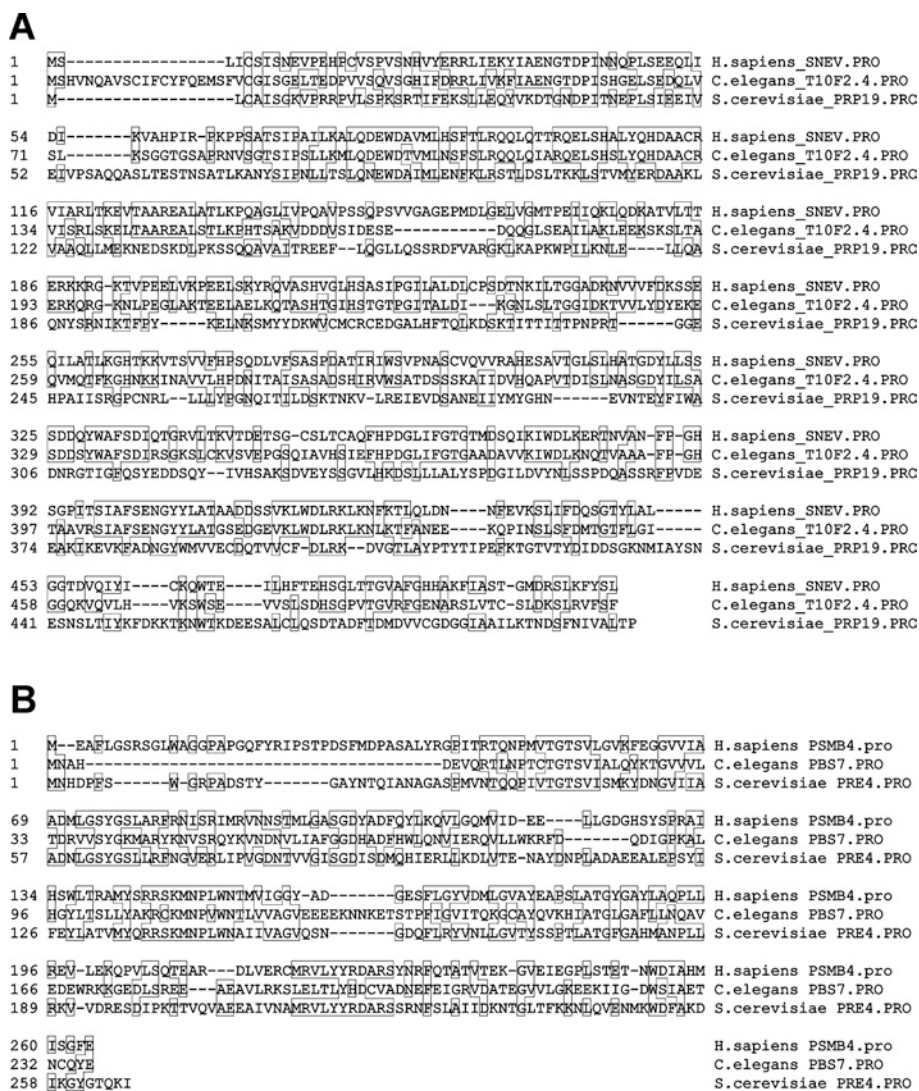


Figure 1 SNEV and the $\beta 7$ subunit of the proteasome are evolutionarily conserved

(A) Sequence comparison of the homologous proteins SNEV (*H. sapiens*), T10F2.4 (*C. elegans*) and Prp19 (*S. cerevisiae*). (B) Sequence comparison of the homologous $\beta 7$ subunits of the 20 S proteasome PSMB4 (*H. sapiens*), pbs7 (*C. elegans*) and Pre4 (*S. cerevisiae*). Homology of SNEV and Prp19 by sequence comparison (BLAST database) revealed 23% (104/439) identities and 41% (184/439) positives; the last 81 (SNEV) or 99 (Prp19) amino acids were not matched. Homology of SNEV and T10F2.4 revealed 50% (253/505) identities and 67% (340/505) positives; the first 17 amino acids of T10F2.4 did not match. PSMB4 and Pre4 showed homology of 43% (100/232) identities and 64% (151/232) positives; the first 41 (PSMB4) or 29 (Pre4) amino acids are not included in the alignment. Homology of PSMB4 and pbs-7 revealed 33% (79/237) identities and 56% (134/237) positives; the first 41 (PSMB4) amino acids are not included in the alignment.

in PBS with 1% goat serum and washed three times for 10 min with PBS. Antibodies used were rabbit anti-SNEV antibody Prp19-867, anti-ubiquitin and anti-proteasome $\alpha 2$ subunit (Affiniti Research). As secondary antibodies, tetramethylrhodamine β -isothiocyanate-labelled anti-mouse antibody and FITC-labelled anti-rabbit antibody (Jackson Immunoresearch Laboratories, West Grove, PA, U.S.A.) were used. Microscopy and image analysis was performed using a Zeiss Delta Vision Restoration microscope as described previously [21].

RESULTS

Interaction of SNEV and Prp19 with the $\beta 7$ subunit of the 20 S proteasome is evolutionarily conserved

In an attempt to further characterize SNEV, we found that its *C. elegans* homologue has been observed to bind to the $\beta 7$ subunit of the *C. elegans* proteasome in a high-throughput Y2H screening

[12]. The corresponding human and yeast genes are evolutionarily conserved (Figure 1A) as shown by sequence comparison of human SNEV with *S. cerevisiae* Prp19 (23% identical and 41% similar amino acids), and with *C. elegans* T10F2.4 (50% identical and 67% similar amino acids). Similarly, human PSMB4 is conserved in comparison with *S. cerevisiae* Pre4 (43% identical and 64% similar amino acids) and with *C. elegans* pbs-7 (33% identical and 56% similar amino acids; Figure 1B). Interestingly, although the human to worm homologue of SNEV seems evolutionarily closer than to the yeast protein, homology of human PSMB4 to the *S. cerevisiae* Pre4 is higher than to *C. elegans* pbs-7.

Because of these homologies, we were interested to know if the interaction between these proteins is also conserved. In a first attempt to test a possible interaction of SNEV and Prp19 with the $\beta 7$ subunit of the proteasome (PSMB4 and Pre4), Y2H experiments were performed. The cDNAs coding for the proteins of

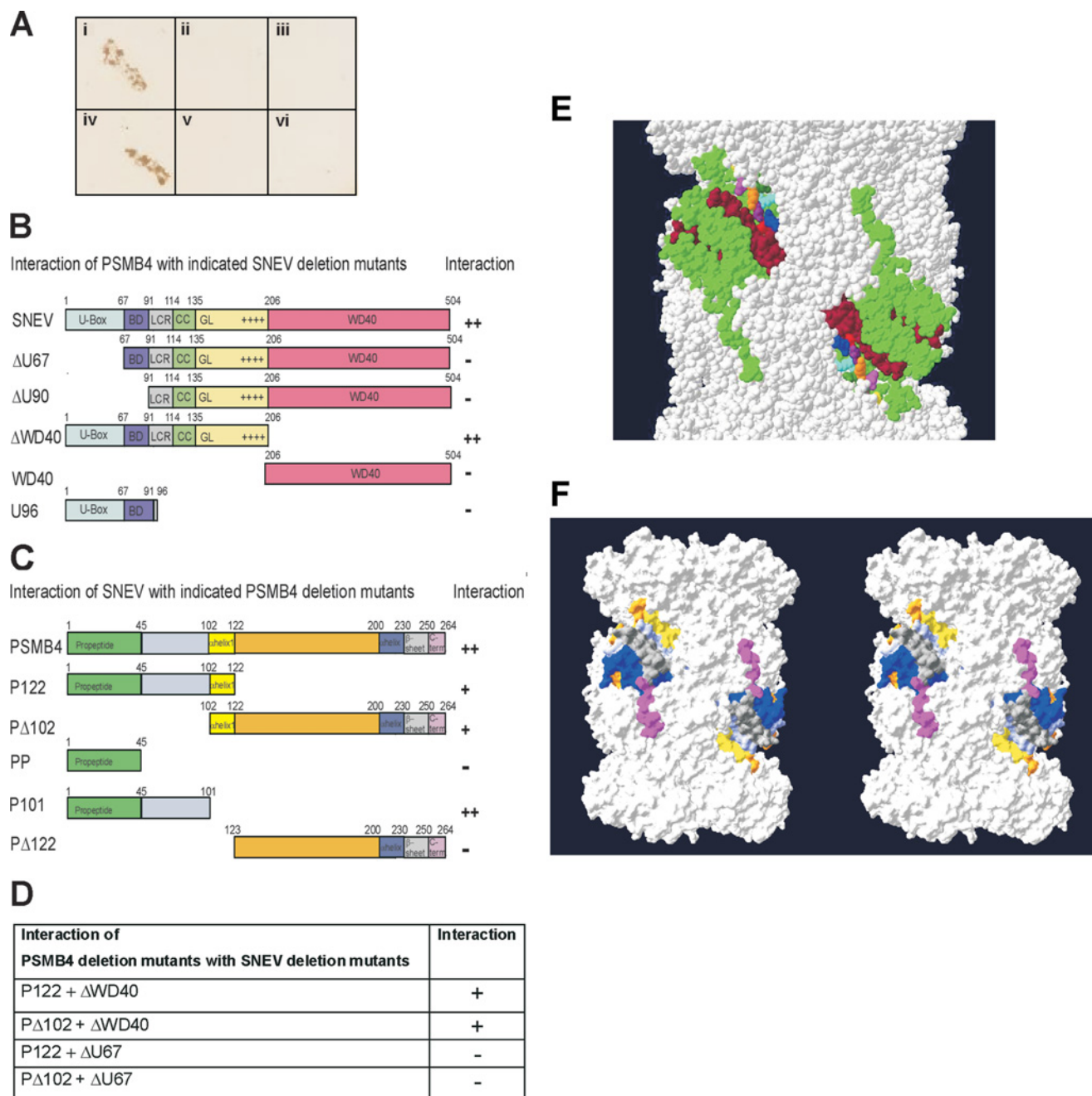


Figure 2 The interaction of SNEV and PSMB4 is evolutionarily highly conserved

(A) Directed Y2H assay for interaction of PRP19 and Pre4 as well as SNEV and PSMB4. The coding sequences were inserted in frame with the GAL4 AD and DNA BD respectively and co-transformed into *S. cerevisiae* AH109. Colony formation on 4 \times dropout medium was observed for SNEV(BD) and PSMB4(AD) (iv) in comparison with control co-transformations of SNEV(BD) and pGADT7 vector alone (v) and PSMB4(AD) and pGBKT7 vector alone (vi). The same result was seen for Prp19(AD) and Pre4(BD) (i) as opposed to the control experiments Pre4(BD) and pGADT7 vector, or Prp19(AD) and pGBKT7 vector (iii). (B, C) Y2H domain mapping of the interacting domains of SNEV and PSMB4. Y2H experiments with the deletion mutant constructs were performed as described in the text. Yeast colonies grown on 4 \times dropout medium (SD-4 \times) were re-streaked on SD-4 \times . ++, >80% of restreaked colonies grew again; -, <80% of restreaked colonies grew again; +, >80% of restreaked colonies grew again, but very slowly (smaller colonies were not visible until 14 days of incubation). (D) Additional Y2H experiments confirming the results of the domain mapping. (E) Calotte model of yeast Pre4 subunit structure (green) in the context of the proteasome (modified from protein database PDB accession no. 1FNT; Rasmol version 2.6). Putative interacting amino acids from the N-terminus of the mature subunit to amino acid 89 are coloured claret red. Putative interacting amino acids of the α -helix 1 region (amino acids 90–108), which are exposed to the surface are coloured: red, M93; blue, Q94; violet, E97; cyan, R98; orange, K101; dark green, D102; purple, V104; black, T105; yellow, A108. Since the α -helix 1 is highly conserved, we presume that these amino acids are also exposed in the mammalian proteasome. (F) surface model of the bovine β 7 subunit incorporated into the proteasome (modified from protein database PDB accession no. 1IRU). Stereo pictures with Swiss PDB viewer version 3.7, peptides coloured as in Figure 2(C).

interest were genetically fused to the GAL4 AD or to the GAL4 BD. After co-transformation of yeast strain AH109 with vectors containing Prp19 and Pre4 or containing SNEV and PSMB4, interaction of SNEV with PSMB4 and of Prp19 with Pre4 (Fig-

ure 2A, iv and i) was indicated by growth on high stringency selection medium. No growth was observed with either of the proteins and the respective second vector containing only the GAL4 AD or BD alone (Figure 2A, ii, iii, v and vi).

Since our main interest lies in the mammalian proteins, further characterization of the domains necessary for their interaction was performed only with SNEV and PSMB4. Different deletion mutants of SNEV were generated for Y2H experiments and were tested by co-transformation with PSMB4 (Figure 2B). Only constructs containing the 68 N-terminal amino acids of SNEV resulted in growth of co-transformed yeast, indicating that these amino acids are necessary for the interaction. Interestingly, this domain corresponds to the U-box of SNEV, which is also necessary for the E3 ligase activity of SNEV [9]. However, although this domain is necessary, it is not sufficient for the interaction. The U96 mutant of SNEV containing only the amino acids 1–96 does not give rise to the formation of yeast colonies.

For PSMB4, the propeptide (1–45) as well as the amino acids from 123–264 (PΔ122) were excluded from containing the binding site of SNEV. The amino acids from 1–101 (P101) however were sufficient for binding to SNEV, suggesting that the binding site maps on to the region from amino acids 46 to 101. However, the α -helical region (α -helix 1) between amino acids 102 and 122 seems to contribute to the interaction, since the construct PΔ102 containing this site interacts with SNEV (Figure 2C), although weakly, as indicated by the decreased growth rate of the positive transformants on high stringency selection medium. However, the fact that the P122 deletion mutant seems to interact more weakly than P101 lacking the α -helix is surprising. We suggest that although this α -helix contributes to the interaction, its presence alone (lacking the C-terminal half of PSMB4) might interfere with folding or accessibility of the interaction site contained in the region 45–101. This hypothesis is supported by the fact that interaction with full-length PSMB4 (containing the C-terminal half) is similar to the interaction of P101 alone.

These results were also confirmed by co-transformation of the two PSMB4 deletion mutants, P122 and PΔ102, and the two SNEV deletion mutants, ΔWD40 and ΔU67 (Figure 2D). The SNEVΔWD40 construct showed the same weak interaction with both PSMB4 constructs as the full-length PSMB4, whereas SNEVΔU67 showed no interaction with either of the two PSMB4 deletion mutants.

To test if the putative interacting amino acids of PSMB4 as determined by Y2H domain mapping are on the outer surface of the proteasome and thus accessible for SNEV interaction, we visualized the region from amino acid 46 to the α helix 1 region within the structure of the proteasome. Therefore we used the models of the yeast and bovine proteasomes [2]. Of these, the bovine structure is the most similar (β 7 subunit: 99% conservation to PSMB4) to the human proteasome. Structure of the mature yeast proteasome has been modelled by RasMol 2.6-beta-2 (Figure 2E) whereas that of the mature bovine proteasome was modelled by Swiss-PdbViewer 3.7 (Figure 2F). The surface-exposed amino acids of the region from amino acid 46 to α -helix 1 of the β 7 subunit integrated into the proteasome are coloured and show that interaction of either SNEV or Prp19 with the mature proteasomes is structurally possible and is consistent with our co-precipitation of SNEV with the proteasome. Domains of the bovine β 7 subunit were coloured like the domains of PSMB4, indicated in Figure 2(C).

Interaction of *in vitro* translated SNEV and PSMB4

To exclude the possibility that the interactions observed by the Y2H system are false positives, we verified our results by CoIP experiments.

For *in vitro* CoIP of SNEV and PSMB4, the proteins were *in vitro* translated as radiolabelled fusions to the Myc and HA tag, using rabbit reticulocyte lysates. After incubation with anti-

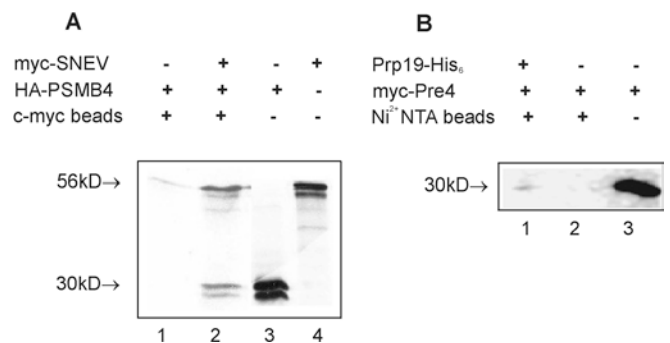


Figure 3 Interaction of *in vitro* translated SNEV and Prp19 with the β 7 subunit of the proteasome

(A) SNEV and PSMB4 were *in vitro* translated as fusions to the Myc- and HA-tag respectively and labelled with ³⁵S-methionine. Precipitation of Myc-tagged SNEV by anti-Myc antibody-coupled beads resulted in co-precipitation of HA-tagged PSMB4 as revealed by SDS/PAGE and autoradiography. Lane 1, negative control, HA-PSMB4 on c-Myc beads; lane 2, CoIP of Myc-SNEV and HA-PSMB4; lane 3, input of *in vitro* translated HA-PSMB4; lane 4, input of *in vitro* translated Myc-SNEV in co-precipitation. (B) Prp4, *in vitro* translated as fusion to the c-Myc-tag, and Prp19-His₆, recombinantly expressed in yeast, were incubated together, followed by incubation with Ni²⁺-NTA beads. Beads were washed and SDS/PAGE was performed. Precipitated Myc-Pre4 was detected with anti-c-Myc antibody. Lane 1, CoIP of Prp19-His₆ and Myc-Pre4, lane 2, Myc-Pre4 on Ni²⁺-NTA beads as negative control and lane 3, input of *in vitro* translated Myc-Pre4 in CoIP.

Myc antibody-coupled beads and three washing steps, SDS/PAGE was performed, and radiolabelled proteins were detected by autoradiography (Figure 3A). HA-tagged PSMB4 was co-precipitated with c-Myc-tagged SNEV on c-Myc-coupled beads, while no PSMB4 was detected in the control, where PSMB4 was incubated with c-Myc beads without SNEV.

Interaction of the yeast partners was similarly confirmed using *in vitro* translated Myc-Pre4 and Prp19-His₆, which was ectopically expressed in *S. cerevisiae*. Precipitation of Prp19-His₆ on Ni²⁺-NTA beads resulted in co-precipitation of Myc-Pre4 as detected by anti-c-Myc antibody. No signal was detected when Pre4 was incubated with Ni²⁺-NTA beads in the absence of Prp19-His₆ (Figure 3B). Therefore we conclude that the interaction between the homologous proteins of SNEV and Prp19 with the respective β 7 proteasome subunits is evolutionarily conserved.

Interaction of SNEV and PSMB4 is direct

CoIP using rabbit reticulocyte lysate does not exclude the possibility that other factors could mediate the observed interaction as bridging factors. Therefore we performed pull-down assays using bacterially expressed PSMB4 as GST fusion protein, together with Ni²⁺-NTA affinity-purified His₆-SNEV produced in insect cells. Only a single band was visible in silver-stained gels of the purified His₆-SNEV (results not shown). Incubation of these purified proteins with GST-Sepharose beads resulted in the precipitation of His₆-SNEV, whereas neither incubation with GST on beads nor with glutathione-beads alone was able to pull down SNEV. Precipitated SNEV was detected using anti-His₄ antibody and GST was detected using anti-GST antibody (Figure 4).

SNEV interacts with the proteasome *in vivo*, but is not degraded by the proteasome

To confirm the *in vivo* relevance of the interaction of SNEV with the proteasome, we tested if endogenous SNEV is detectable in proteasome isolations. Therefore we precipitated the proteasomes from HEK-293 cell lysates using anti- α 2 subunit antibodies coupled with Protein A beads. Indeed, SNEV was detected in the precipitate, in contrast with precipitates using Protein A beads

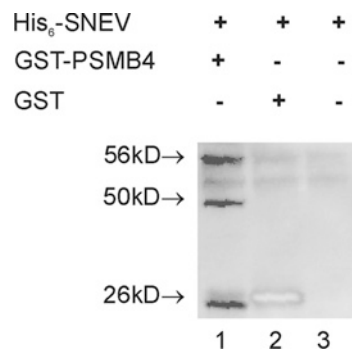


Figure 4 The interaction of SNEV and PSMB4 is direct

Purified GST-PSMB4 fusion protein expressed in *E. coli* was incubated together with affinity-purified His₆-SNEV, expressed by baculovirus/insect cell system and precipitated on GST-Sepharose beads. The precipitate was separated by SDS/PAGE and detected by Western blot. SNEV was detected by anti-His₆ antibody. As control, GST and GST-PSMB4 were detected with anti-GST antibody. Lane 1, CoIP of GST-PSMB4 (without propeptide, 50 kDa) and His₆-SNEV (56 kDa) on GST-beads; lane 2, CoIP of GST (26 kDa) alone and His₆-SNEV on GST-beads [image acquired by Lumilmager (Roche); since the GST signal is too strong, it is displayed as inverted]; lane 3, His₆-SNEV alone on GST-beads.

charged with the irrelevant anti-c-Myc antibody (Figure 5A). In these precipitations, only a portion of SNEV seems proteasome-associated, as can be observed when comparing SNEV amounts contained in the precipitated proteasome with those contained in the total cell lysates.

The interaction with the proteasome might indicate that SNEV is degraded by this major proteolytic machinery. Therefore we treated HeLa cells for 6 h with the proteasome inhibitor MG132 and analysed the amount of SNEV protein on Western blots (Figure 5B). Blocking of proteasome activity was monitored by accumulation of ubiquitinated protein species in the cell lysates, as well as by accumulation of the proteasome substrate p53. In contrast, no significant increase in the protein levels of SNEV and β -actin (as protein loading control) was visible. In line with this result, no additional higher molecular mass band or smear that could represent accumulation of mono- or multi-ubiquitinated SNEV was detected using anti-SNEV antibodies.

Additional evidence that SNEV might not be a substrate to the proteasome is derived from *in vitro* experiments. When active purified proteasome was added to recombinant SNEV, no difference in SNEV degradation with or without 26 S proteasome was observed on Western blots, which were quantified by densitometry (Figure 5C). Activity of the proteasome preparation was controlled by using I κ B α as substrate, which was readily degraded. These results suggest that SNEV is, at least under the conditions tested, not a substrate for proteasomal degradation. This is consistent with the pulse-chase labelling experiment by Gotzmann et al. [7], who have shown that SNEV amounts do not decrease in Jurkat cells during 24 h of observation.

Since SNEV is reported to be contained in a multiprotein complex, we also tested another protein in this complex, Cdc5L [6], in our proteasome precipitations (Figure 5A). Indeed, we were able to detect Cdc5L, indicating that at least one other protein of the Cdc5L-associated complex interacts with the proteasome. It should be noted, however, that no proteasomal subunits were found in a screening for proteins that co-precipitate together with the Cdc5L-associated complex [6].

FRET analysis

As an additional confirmation and to localize the interaction of SNEV and PSMB4 within the cells, we inserted the cDNAs into

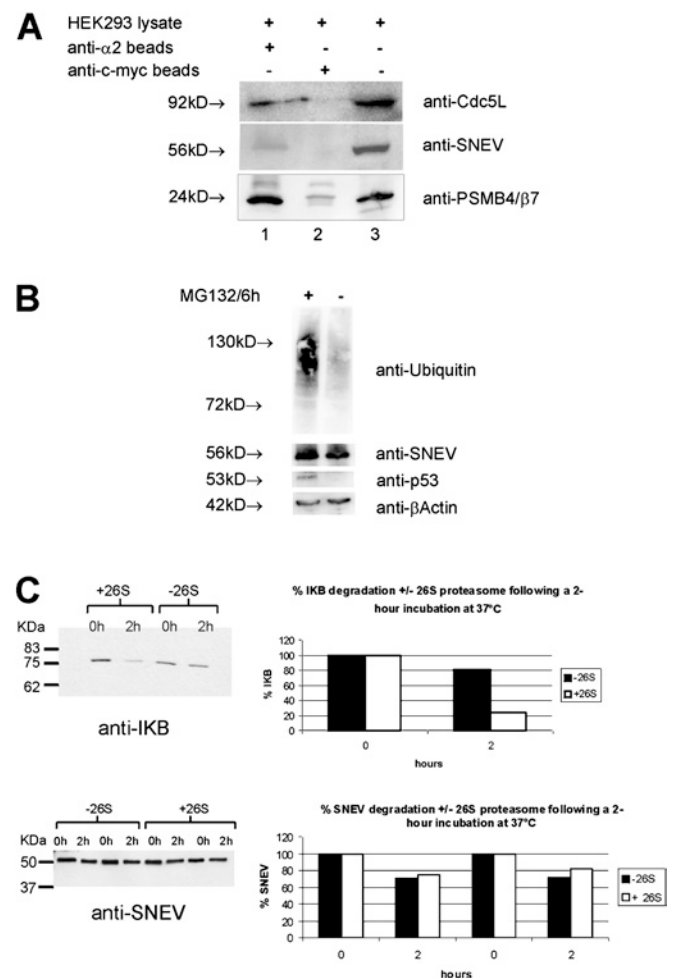


Figure 5 SNEV interacts with the proteasome *in vivo* but is not degraded by it

(A) Proteasome was precipitated from HEK-293 cell lysate by anti- α 2-coupled Protein A beads. After washing the beads and elution of proteins by resuspending the beads in SDS-loading buffer, SDS/PAGE was performed. Precipitation of the proteasome was confirmed on Western blots with anti-PSMB4 antibody, whereas co-precipitated SNEV was detected with anti-SNEV antibody. Lane 1, mouse-anti- α 2 antibody-coupled beads co-precipitate PSMB4 and SNEV; lane 2, mouse-anti-Myc antibody-coupled beads were used as negative control, cell lysate on anti-c-Myc-coupled beads; lane 3, whole cell lysate as input control. (B) Western blot of HeLa cell extracts that were treated with 25 μ M MG132 for 6 h (+) versus untreated controls (-). Protein amounts of SNEV and β -actin do not change, indicating that SNEV is not a substrate to the proteasome. To control the effect of MG132 on the cells, we probed for p53, a known proteasomal substrate, and for polyubiquitinated proteins, using anti-p53 and anti-ubiquitin antibodies respectively. Indeed, both p53 and ubiquitinated proteins accumulate on proteasome inhibition. (C) *In vitro* 26 S proteasome degradation assay. SNEV was incubated with or without the 26 S proteasome for 0 and 2 h in an *in vitro* degradation assay. Quantification of SNEV protein amounts detected on Western blots was achieved by densitometry. As positive control for the *in vitro* degradation assay, I κ B α was used as the model substrate and detected in a Western blot by anti-I κ B α antibody. Although only 80% of SNEV was detected after incubation for 2 h at 37°C, this degradation was not dependent on the addition of the 26 S proteasome, suggesting that SNEV is not a substrate of the proteasome.

pECFP and pEYFP vectors (Figure 6). After co-transformation of two different cell lines (COS-1 and HEK-293), interaction between these proteins was observed by MicroFRET analysis [22] in living cells. The interaction was primarily localized within the cytoplasm, but a fainter FRET signal was also detected in the nucleus. As negative controls, we used Δ 66-SNEV, which lacks the U-box that is necessary for the interaction in the Y2H experiments, as well as Δ 89-SNEV. On co-transfection with PSMB4, no FRET signal was observed (Figures 6P and 6R), similar to

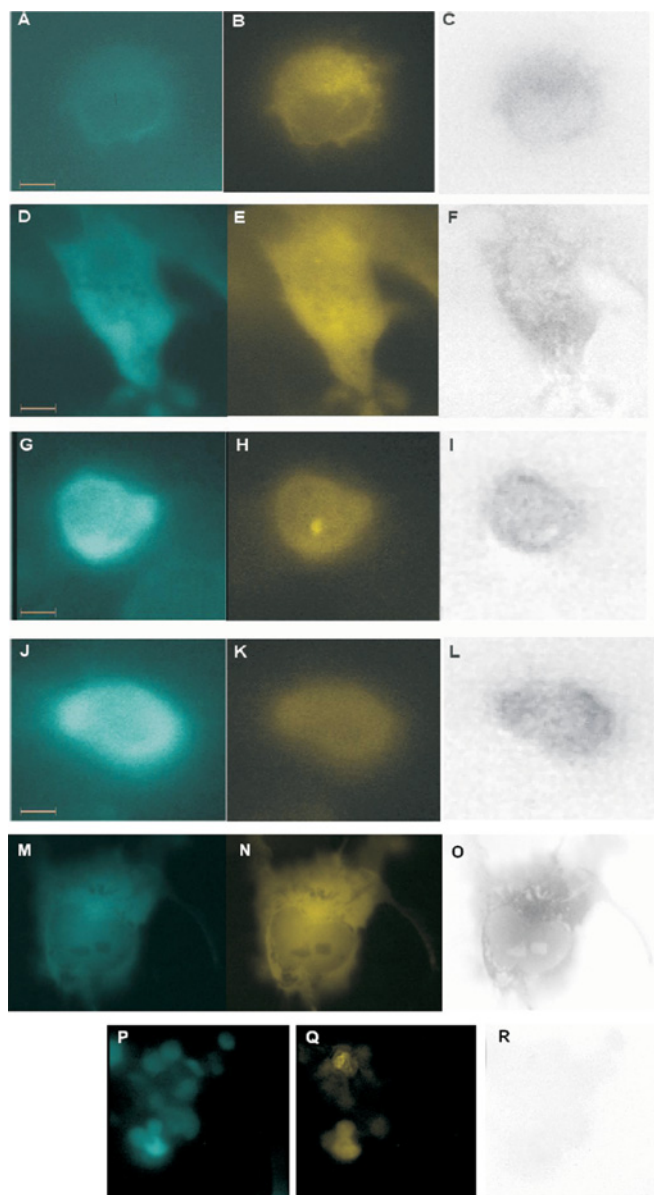


Figure 6 Interaction of SNEV and PSMB4 can be visualized in cells by FRET

COS-1 (**A–F**) and HEK-293 cells (**G–L**) were co-transfected with plasmids carrying SNEV, N-terminally fused to ECFP (cyan), and PSMB4, C-terminally fused to EYFP (yellow). **A, D, G, J**: microscopic picture using CFP-filter (SNEV); **B, E, H, K**: picture using YFP-filter (PSMB4) and **C, F, I, L**: calculated net FRET signal of SNEV and PSMB4. Scale bar, 10 μm ($\times 60$ objective). **M–O**: Positive control using an EYFP–ECFP fusion protein in COS-1 cells. **P–R**: Negative control using HEK-293 cells co-transfected with plasmids coding for ECFP– $\Delta 66$ -SNEV and PSMB4–EYFP fusion proteins. The pictures (**P–R**) were taken using a lower magnification ($\times 40$ objective).

the co-transfection of SNEV–ECFP (enhanced CFP) and unfused EYFP (enhanced YFP; results not shown). As positive control, an EYFP–ECFP fusion protein was used (Figures 6M and 6O).

These results, however, have several limitations. An ECFP–SNEV fusion protein was found in the cytoplasm and nucleus, whereas the endogenous protein is mainly found in the nucleus (J. Grillari and R. Voglauer, unpublished work and [7]). Additionally, PSMB4–EYFP fusion proteins did not integrate into mature proteasomes. We were not able to detect the fusion protein in proteasome precipitations from HEK-293 cells transiently transfected with pEYFP–PSMB4 (results not shown), a result

consistent with the observation of Lin et al. [23] who showed that C-terminally FLAG-tagged PSMB4 is also not integrated into the proteasome.

Finally, the cellular localization of SNEV was altered either by fusion to ECFP, by overexpression or by the interaction with free PSMB4–EYFP that might interfere with the import of SNEV into the nucleus. Therefore although our FRET analysis confirms an interaction of the recombinant proteins in living cells, it seems to have no relevance for the real localization.

Co-localization of SNEV with the proteasome and ubiquitin

Since the FRET experiment did not reveal in which cellular compartment the interaction between SNEV and the proteasome is likely to occur, we performed indirect immunofluorescence experiments using antibodies against the endogenous proteins in HeLa cells for co-localization. Since we reasoned that the E3 ligase SNEV might transport the target of its ubiquitination activity to the proteasome and after ‘delivery’ might quickly dissociate again, we included HeLa cells treated with the proteasome inhibitor MG132 in this analysis. We observed rare co-localization of SNEV with the proteasome without MG132 (Figures 7A–7C), consistent with a low amount of SNEV in proteasome precipitates, but a marked increase in co-localizing speckle-like structures with proteasome inhibition (Figures 7D–7F). When we tested SNEV and ubiquitin for co-localization, the staining of ubiquitin was very weak in untreated HeLa cells (results not shown), but was clearly co-localizing with SNEV in MG132 treated cells in similar speckle-like structures as SNEV and the proteasome (Figures 7G–7J).

These results, in combination with our result that neither the total amount of SNEV nor that of ubiquitinated SNEV increases on proteasome inhibition, suggests that SNEV might display E3 ligase activity not only *in vitro* but also *in vivo* and that it might transport its ubiquitinated substrate to the proteasome, presumably for degradation.

DISCUSSION

By a subtractive hybridization method, various differentially expressed genes were identified from early passage and senescent HUVECs [5]. One of these genes, the unknown gene 4, now termed SNEV, was selected for further characterization. The mRNA encoding the putative protein SNEV is present in all human tissues tested (kidney, lung, placenta, small intestine, liver, peripheral blood leucocytes, spleen, thymus, colon, skeletal muscle, heart and brain), and no alternative splicing products have been identified (J. Grillari, unpublished work; [7]).

SNEV is a multifaceted protein that is involved in DNA double-strand break repair [8], in splicing [6] and life span extension (R. Voglauer, W. M. F. Chang, M. Wieser, K. Baumann, H. Katinger and J. Grillari, unpublished work).

Within the first 68 amino acids, a U-box [a modified RING (really interesting new gene) finger] domain was identified by SMART search. This conserved domain is found in a large variety of proteins that show E3 ligase activity [24]. Indeed, Hatakeyama et al. [9] have shown that SNEV has E3 ligase activity *in vitro*, when tested with Ubc3 (cdc34) as E2 enzyme, and that the ubiquitin transfer is dependent on the U-box [9]. Additionally, SNEV has been shown to mediate multiubiquitination through the Lys⁴⁸ residue [9], which is known to target substrates to the proteasome [1,4].

Different E3 ligases have been reported to physically interact with the proteasome, like the yeast proteins Ubr1p, a RING-H2 domain containing protein, and Ufd4p, a HECT (homology to

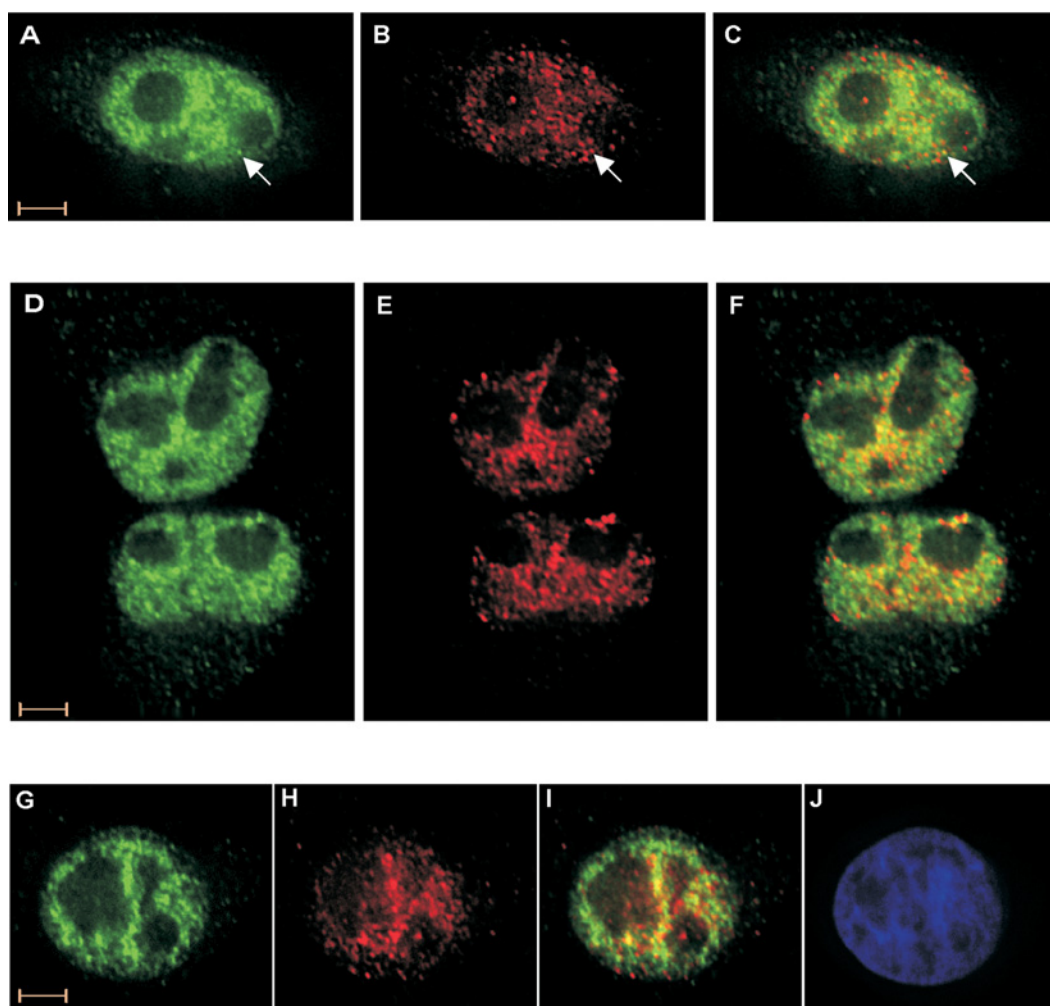


Figure 7 Partial nuclear co-localization of SNEV with the proteasome and with ubiquitin in HeLa cells after MG132 treatment

HeLa cells were treated with DMSO as control (**A–C**) and with 25 μ M MG132 (dissolved in DMSO) for 6 h. Indirect immunofluorescence was performed using anti-SNEV (green, **A, D**) and anti- α 2 proteasome subunit antibodies (red, **B, E**). Overlay of these pictures shows partial co-localization (yellow) of SNEV and the proteasome, which is rare in untreated (**C**, yellow spot indicated by arrow) versus proteasome-inhibited cells (**F**). Co-localization was also observed between SNEV (**G**, green) and ubiquitin (**H**, red), as can be seen in the overlay (**I**), although only in MG 132-treated cells. (**J**) Representative DAPI staining for visualization of the nucleus. Scale bar, 5 μ m.

E6-AP C-terminal)-domain E3 ligase [11]. Additional evidence for an interaction between ubiquitin-conjugating enzymes and the 26 S proteasome in yeast is derived from the report that various E3 ligases also interact with the proteasome [25]. In mammalian cells, however, only the von Hippel-Lindau protein, a component of the von Hippel-Lindau-Elongin B/C-cullin 2 (VEC) E3 ligase complex, has been shown to interact with the proteasome [26]. All of these proteins bind to components of the 19 S lid of the proteasome.

To verify if an interaction of our E3 ligase SNEV with the proteasome can be observed, we looked for potential proteasomal interactors. Thereby, we found a putative candidate that was identified in a high-throughput Y2H study. Putative interaction between T10F2.4, the *C. elegans* homologue of SNEV, and F39H11.5, the β 7 subunit of the proteasome, was reported ([12], electronic supplement).

In the present study, we have shown that SNEV indeed interacts directly with PSMB4 *in vitro* by different independent methods and that this interaction is conserved from yeast to mammalian cells. Additionally, proteasome precipitates contain endogenous SNEV protein, indicating that a portion of SNEV is associated

with the proteasome *in vivo* and strongly suggesting that this association is dependent on binding to PSMB4.

Results of the present study are supported by indirect immunofluorescence experiments, where SNEV partially co-localizes with the proteasome. When the cells are treated with the proteasome inhibitor MG132, this co-localization increases significantly. Co-localizations of SNEV with the proteasome or with ubiquitin that we have observed occur in nuclear speckle-like structures. Similar structures, termed clastosomes, have already been described to contain ubiquitin conjugates, protein substrates and proteasomes [27].

These findings suggest that either SNEV itself is a substrate of proteasomal degradation, or that SNEV as an E3 ligase escorts its substrate(s) to the proteasome and accumulates there, since ‘delivery’ and in turn dissociation fails due to proteasome inhibition. The latter hypothesis is supported by the fact that SNEV does not accumulate within the cells on inhibition of the proteasome and that no additional bands indicating SNEV ubiquitination are detected on Western blots. Additionally, SNEV is not degraded by the 26 S proteasome, when tested *in vitro*. However, ubiquitin does co-localize with SNEV on proteasome

inhibition, suggesting that SNEV might have E3 ligase activity not only *in vitro* [9], but also *in vivo*.

There are several reports available on the function of homologous yeast and human subunits of the 20 S proteasome Pre4 and PSMB4. For the yeast subunit Pre4, these results are mainly derived from genetic mutant strains. Pre4 is located within the inner ring of the 20 S proteasome and is a crucial component in assembling the proteasome [28]. Two yeast mutant strains with defects in Pre4 are presently known. Pre4-1 mutants show a defect in peptidyl glutamyl peptide hydrolase activity of the proteasome [29] and, like several other mutants of proteasome subunits, are resistant to cycloheximide [30]. Pre4-2 mutants suppress a mutation of mitochondrial RNase P that leads to lack of growth on fermentative carbon sources [31]. Another protein that is functionally connected to Pre4 is Sit4 phosphatase, the concerted action of which is necessary for cell maintenance during starvation-induced G1 arrest [32].

The human protein PSMB4 is known mainly as an interaction partner for several proteins, suggesting an important function of binding not only to the lid, but also to the 20 S core of the proteasome. The HIV-derived protein Nef1 binds to the amino acids 73–249, where the amino acids 219–249 are of major importance, although not sufficient [33]. Another viral protein binding to PSMB4 is Tax (human T-cell leukaemia virus), an interaction that is supposed to influence the nuclear factor κ B pathway [34].

Signalling of the transforming growth factor β superfamily is also influenced by binding of Smad1 to PSMB4 (reviewed in [35]), an interaction that occurs with the immature half proteasomes [36]. This is in contrast with SNEV–proteasome interaction that occurs with the mature proteasome, since we do not detect unprocessed PSMB4 in our precipitates, but only the mature form at 24 kDa.

Other interacting partners of PSMB4 are lipopolysaccharides of microbial origin, which have been shown to influence the activity of the proteasome by increasing the chymotrypsin-like activity on binding to PSMB4 [37].

These reports together with our results suggest that PSMB4 might be a major site for proteasome regulation, where signals from the outside might be transduced to the protease activities inside. However, we were not able to detect changes in proteasome activity on addition of recombinant SNEV *in vitro* (results not shown).

Although this is the first report showing that a U-box E3 ligase binds to the proteasome and that this binding is not directed to the lid but to the core, co-localization of nuclear proteins, especially of splicing factors, that are targets of proteasomal degradation has already been observed [38]. Since SNEV is also contained within the spliceosome [6], these results suggest that SNEV might be involved in the degradation of spliceosomal proteins to allow the large structural rearrangements that are necessary for spliceosome activation and splicing catalysis. However, SNEV is also reported to be involved in DNA double-strand break repair [8] and it is presently not clear which of these functions is dependent on the enzymatic activity of SNEV in the ubiquitin–proteasome degradation pathway. We will get closer to answering this question as soon as the target of SNEV's E3 ligase activity has been identified.

We are grateful to Polymun Scientific, Vienna for generous funding of this project. W. Ernst provided baculovirally expressed SNEV protein. We thank N. Chondrogianni for helpful discussions.

REFERENCES

- Ciechanover, A. and Schwartz, A. L. (1998) The ubiquitin–proteasome pathway: the complexity and myriad functions of protein death. *Proc. Natl. Acad. Sci. U.S.A.* **95**, 2727–2730
- Unno, M., Mizushima, T., Morimoto, Y., Tomisugi, Y., Tanaka, K., Yasuoka, N. and Tsukihara, T. (2002) The structure of the mammalian 20 S proteasome at 2.75 Å resolution. *Structure* **10**, 609–618
- Ferrell, K., Wilkinson, C. R., Dubiel, W. and Gordon, C. (2000) Regulatory subunit interactions of the 26 S proteasome, a complex problem. *Trends Biochem. Sci.* **25**, 83–88
- Weissman, A. M. (2001) Themes and variations on ubiquitylation. *Nat. Rev. Mol. Cell. Biol.* **2**, 169–178
- Grillari, J., Hohenwarter, O., Grabherr, R. M. and Katinger, H. (2000) Subtractive hybridization of mRNA from early passage and senescent endothelial cells. *Exp. Gerontol.* **35**, 187–197
- Ajuh, P., Kuster, B., Panov, K., Zomerdijk, J. C., Mann, M. and Lamond, A. I. (2000) Functional analysis of the human CDC5L complex and identification of its components by mass spectrometry. *EMBO J.* **19**, 6569–6581
- Goltzmann, J., Gerner, C., Meissner, M., Holzmann, K., Grimm, R., Mikulits, W. and Saueremann, G. (2000) hNMP 200: a novel human common nuclear matrix protein combining structural and regulatory functions. *Exp. Cell. Res.* **261**, 166–179
- Mahajan, K. N. and Mitchell, B. S. (2003) Role of human Pso4 in mammalian DNA repair and association with terminal deoxynucleotidyl transferase. *Proc. Natl. Acad. Sci. U.S.A.* **100**, 10746–10751
- Hatakeyama, S., Yada, M., Matsumoto, M., Ishida, N. and Nakayama, K. I. (2001) U-Box proteins as a new family of ubiquitin–protein ligases. *J. Biol. Chem.* **276**, 33111–33120
- Xie, Y. and Varshavsky, A. (2002) UFD4 lacking the proteasome-binding region catalyses ubiquitination but is impaired in proteolysis. *Nat. Cell Biol.* **4**, 1003–1007
- Xie, Y. and Varshavsky, A. (2000) Physical association of ubiquitin ligases and the 26 S proteasome. *Proc. Natl. Acad. Sci. U.S.A.* **97**, 2497–2502
- Davy, A., Bello, P., Thierry-Mieg, N., Vaglio, P., Hitti, J., Doucette-Stamm, L., Thierry-Mieg, D., Reboul, J., Boulton, S., Walhout, A. J. et al. (2001) A protein–protein interaction map of the *Caenorhabditis elegans* 26 S proteasome. *EMBO Rep.* **2**, 821–828
- Altschul, S. F., Gish, W., Miller, W., Myers, E. W. and Lipman, D. J. (1990) Basic local alignment search tool. *J. Mol. Biol.* **215**, 403–410
- Guex, N. and Peitsch, M. C. (1997) SWISS-MODEL and the Swiss-PdbViewer: an environment for comparative protein modeling. *Electrophoresis* **18**, 2714–2723
- Sayle, R. A. and Milner-White, E. J. (1995) RASMOL: biomolecular graphics for all. *Trends Biochem. Sci.* **20**, 374
- Maniatis, T., Fritsch, E. F. and Sambrook, J. (1987) *Molecular Cloning: A Laboratory Manual*, Cold Spring Harbor Laboratory Press, Plainview, NY
- Gietz, R. D., Triggs-Raine, B., Robbins, A., Graham, K. C. and Woods, R. A. (1997) Identification of proteins that interact with a protein of interest: applications of the yeast two-hybrid system. *Mol. Cell. Biochem.* **172**, 67–79
- Reference deleted
- Reidlinger, J., Pike, A. M., Savory, P. J., Murray, R. Z. and Rivett, A. J. (1997) Catalytic properties of 26 S and 20 S proteasomes and radiolabeling of MB1, LMP7, and C7 subunits associated with trypsin-like and chymotrypsin-like activities. *J. Biol. Chem.* **272**, 24899–24905
- Youvan, D. C., Silva, C. M., Bylina, E. J., Coleman, W. J., Dilworth, M. R. and Yang, M. M. (1997) Calibration of fluorescence resonance energy transfer in microscopy using genetically engineered GFP derivatives on nickel chelating beads. *Biotechnology* **3**, 1–18
- Platani, M., Goldberg, I., Swedlow, J. R. and Lamond, A. I. (2000) *In vivo* analysis of Cajal body movement, separation, and joining in live human cells. *J. Cell Biol.* **151**, 1561–1574
- Youvan, D. C., Coleman, W. J., Silva, C. M., Petersen, J., Bylina, E. J. and Yang, M. M. (1997) Fluorescence imaging micro-spectrophotometer (FIMS). *Biotechnology* **1**, 1–16
- Lin, Y., Martin, J., Gruendler, C., Farley, J., Meng, X., Li, B. Y., Lechleider, R., Huff, C., Kim, R. H., Grasser, W. A. et al. (2002) A novel link between the proteasome pathway and the signal transduction pathway of the bone morphogenetic proteins (BMPs). *BMC Cell Biol.* **3**, 15
- Aravind, L. and Koonin, E. V. (2000) The U box is a modified RING finger – a common domain in ubiquitination. *Curr. Biol.* **10**, R132–R134 [letter]
- Tongaonkar, P., Chen, L., Lambertson, D., Ko, B. and Madura, K. (2000) Evidence for an interaction between ubiquitin-conjugating enzymes and the 26 S proteasome. *Mol. Cell. Biol.* **20**, 4691–4698
- Corn, P. G., McDonald, E. R., Herman, J. G. and El-Deiry, W. S. (2003) Tat-binding protein-1, a component of the 26 S proteasome, contributes to the E3 ubiquitin ligase function of the von Hippel-Lindau protein. *Nat. Genet.* **35**, 229–237
- Lafarga, M., Berciano, M. T., Pena, E., Mayo, I., Castano, J. G., Bohmann, D., Rodrigues, J. P., Tavanez, J. P. and Carmo-Fonseca, M. (2002) Clastosome: a subtype of nuclear body enriched in 19S and 20S proteasomes, ubiquitin, and protein substrates of proteasome. *Mol. Biol. Cell.* **13**, 2771–2782

- 28 Ramos, P. C., Marques, A. J., London, M. K. and Dohmen, R. J. (2004) Role of C-terminal extensions of subunits $\beta 2$ and $\beta 7$ in assembly and activity of eukaryotic proteasomes. *J. Biol. Chem.* **279**, 14323–14330
- 29 Hilt, W., Enenkel, C., Gruhler, A., Singer, T. and Wolf, D. H. (1993) The PRE4 gene codes for a subunit of the yeast proteasome necessary for peptidylglutamyl-peptide-hydrolyzing activity. Mutations link the proteasome to stress- and ubiquitin-dependent proteolysis. *J. Biol. Chem.* **268**, 3479–3486
- 30 Gerlinger, U. M., Guckel, R., Hoffmann, M., Wolf, D. H. and Hilt, W. (1997) Yeast cycloheximide-resistant *crl* mutants are proteasome mutants defective in protein degradation. *Mol. Biol. Cell.* **8**, 2487–2499
- 31 Lutz, M. S., Ellis, S. R. and Martin, N. C. (2000) Proteasome mutants, *pre4-2* and *ump1-2*, suppress the essential function but not the mitochondrial RNase P function of the *Saccharomyces cerevisiae* gene *RPM2*. *Genetics* **154**, 1013–1023
- 32 Singer, T., Haefner, S., Hoffmann, M., Fischer, M., Ilyina, J. and Hilt, W. (2003) Sit4 phosphatase is functionally linked to the ubiquitin-proteasome system. *Genetics* **164**, 1305–1321
- 33 Rossi, F., Evstafieva, A., Pedrali-Noy, G., Gallina, A. and Milanesi, G. (1997) HsN3 proteasomal subunit as a target for human immunodeficiency virus type 1 Nef protein. *Virology* **237**, 33–45
- 34 Rousset, R., Desbois, C., Bantignies, F. and Jalinot, P. (1996) Effects on NF-kappa B1/p105 processing of the interaction between the HTLV-1 transactivator Tax and the proteasome. *Nature (London)* **381**, 328–331
- 35 Wang, T. (2003) The 26 S proteasome system in the signaling pathways of TGF-beta superfamily. *Front. Biosci.* **8**, d1109-d1127
- 36 Gruendler, C., Lin, Y., Farley, J. and Wang, T. (2001) Proteasomal degradation of Smad1 induced by bone morphogenetic proteins. *J. Biol. Chem.* **276**, 46533–46543
- 37 Qureshi, N., Perera, P. Y., Shen, J., Zhang, G., Lenschat, A., Splitter, G., Morrison, D. C. and Vogel, S. N. (2003) The proteasome as a lipopolysaccharide-binding protein in macrophages: differential effects of proteasome inhibition on lipopolysaccharide-induced signaling events. *J. Immunol.* **171**, 1515–1525
- 38 Rockel, T. and von Mikecz, A. (2002) Proteasome-dependent processing of nuclear proteins is correlated with their subnuclear localization. *J. Struct. Biol.* **140**, 189–199

Received 6 September 2004/21 December 2004; accepted 20 January 2005
Published as BJ Immediate Publication 20 January 2005, DOI 10.1042/BJ20041517